J Comput Aided Mol Des (2008) 22:915–923
DOI 10.1007/s10822-008-9228-1

Structural modeling of glucanase–substrate complexes suggests a conserved tyrosine is involved in carbohydrate recognition in plant 1,3-1,4-β-D-glucanases

Li-Chu Tsai · Yi-Ning Chen · Lie-Fen Shyur

Received: 30 May 2008 / Accepted: 8 July 2008 / Published online: 29 July 2008

Abstract Glycosyl hydrolase family 16 (GHF16) truncated *Fibrobacter succinogenes* (TFs) and GHF17 barley 1,3-1,4-β-D-glucanases (β-glucanases) possess different structural folds, β-jellyroll and $(\beta/\alpha)_8$, although they both catalyze the specific hydrolysis of β-1,4 glycosidic bonds adjacent to β-1,3 linkages in mixed β-1,3 and β-1,4 β-D-glucans or lichenan. Differences in the active site region residues of TFs β-glucanase and barley β-glucanase create binding site topographies that require different substrate conformations. In contrast to barley β-glucanase, TFs β-glucanase possesses a unique and compact active site. The structural analysis results suggest that the tyrosine residue, which is conserved in all known 1,3-1,4-β-D-glucanases, is involved in the recognition of mixed β-1,3 and β-1,4 linked polysaccharide.

Keywords Glycosyl hydrolase · β-1,4-1,3-D-Oligosaccharide · β-1,3-D-Oligosaccharide · Catalytic residues · Families 16 and 17 · Molecular minimization

Introduction

The recognition and hydrolysis of carbohydrate by enzymes is a fundamental biological phenomenon, important to numerous metabolic events including cellular processes, energy uptake, and degradation. Glycosyl hydrolases have the ability to recognize and bind particular carbohydrates and then cleave a specific glycosidic bond between two or more carbohydrates. In addition, glycosyl hydrolases are known to use two major hydrolytic mechanisms, inversion or retention [1, 2]. Over the years the number of families of glycosyl hydrolases known to researchers has grown steadily (http://afmb.cnrs-mrs.fr/CAZY/). Forty-eight families of glycosyl hydrolases have had their three-dimensional structures reported, seven structural folds, namely $(\beta/\alpha)_8$, β-jellyroll, sixfold-β-propeller, fivefold-β-propeller, $(\alpha + \beta)$, $(\alpha/\alpha)_6$, and β-helix, have been proposed to characterize those 48 families on the basis of three-dimensional similarities. Over the years many structural research reports on protein–carbohydrate interaction have made protein–carbohydrate recognition mechanism more clear [3–5].

β-Glucanases (EC 3.2.1.73) hydrolyze and cleave β-1,4-glycosidic bonds precisely where β-1,3-glycosidic linkages are located prior to β-1,4-glycosidic linkages in lichenan or β-D-glucans [6] via a retention cleavage mechanism. β-Glucanases are present in different bacteria, fungi, and plants. Currently, β-glucanases from the bacteria *Bacillus licheniformis*, *Paenibacillus macerans* [7–10] and *Fibrobacter succinogenes* (Fs) [11, 12], and barley β-glucanase [13–15] have received the most attention, with the identification of the two important residues for hydrolysis of the glycosidic bond, a nucleophile and a hydrogen donor. The crystal structure of β-glucanase from bacteria [16, 17] exhibits a jellyroll β-sandwich fold with a cleft active site, classified as glycosyl hydrolase family 16 (GHF16). Barley β-glucanase, which folds into a $(\beta/\alpha)_8$ motif [14, 15] with a pocket active site, is regarded as being a member of GHF17. Although the amino acid sequences and tertiary structures of GHF16 bacterial and GHF17 barley β-glucanases are

L.-C. Tsai (✉)
Department of Molecular Science and Engineering, National Taipei University of Technology, Taipei, Taiwan
e-mail: lichu@ntut.edu.tw

Y.-N. Chen
Institute of Molecular Biology, Academia Sinica, Taipei, Taiwan

L.-F. Shyur
Agricultural Biotechnology Research Center, Academia Sinica, Taipei, Taiwan

unrelated, both enzymes share a similar retention cleavage mechanism (http://afmb.cnrs-mrs.fr/CAZY/).

With the publication of the TFsβ-glucanase-β-1,4-1,3-cellotriose complex structure [16], it was recently revealed how the product β-1,4-1,3-cellotriose (subunits -3 to -1) binds to the enzyme active site. This confirmed our previous studies indicating that residues Glu56 and Glu60 act as the catalytic nucleophile and the hydrogen donor [11], respectively. In addition, Chen and co-workers have reported [13] kinetic studies on GHF17 barley β-glucanase which suggest that its Glu232 and Glu288 residues act analogously to Glu56 and Glu60 in TFsβ-glucanase. In contrast, Jenkins and co-workers later reported that it is instead the Glu232 and Glu93 in barley β-glucanase that act as the catalytic nucleophile and hydrogen donor [18]. Moreover, in another GHF17 structure, that of banana β-1,3-glucanase, it was suggested that the residues Glu236 and Glu94, which are conserved and equivalent to residues Glu232 and Glu93 in barley β-glucanase, act as the catalytic nucleophile and the hydrogen donor, respectively, and a cellotriose-containing (subsites -2 to $+1$) complex model was reported [19]. We used comparative modeling and structural analysis to determine the role of residues Glu93, Glu232, and Glu288 in GHF17 barley β-glucanase.

In this study, we modeled a β-1,3-1,4-cellohexaose (CLHA1) based on β-1,4-1,3-cellotriose [16] into the active site of barley β-glucanase, using Glu232/Glu93 as the nucleophile/hydrogen donor. As a contrast to CLHA1, we also modeled a β-1,3-cellohexaose (CLHA2) into the active site of banana β-1,3-glucanase, based on the previously proposed catalytic nucleophile/hydrogen donor residue pair Glu236/Glu94 [19]. In addition, a cellobiose was added to β-1,4-1,3-cellotriose to mimic a substrate β-1,3-1,4-cellopentose (CLPA) occupying the whole active site of TFsβ-glucanase in a substrate binding affinity analysis. This study addresses how the two different TFsβ-glucanase and barley β-glucanase active site residues interact with lichenan or β-D-glucans (CLPA and CLHA1), and how the two similar active site residues in barley β-glucanase and banana β-1,3-glucanase interact with two different substrates, CLHA1 and CLHA2.

Material and methods

Construction of a cellobiose into the TFsβ-glucanase-β-1,4-1,3-cellotriose complex structure

Coordinates of the published TFsβ-glucanase and β-1,4-1,3-cellotriose complex structures, PDB code 1ZM1 [16], were used for construction of TFsβ-glucanase-CLPA complex. The β-1,4-1,3-cellotriose located in the complex structure was numbered -3 to -1, and occupied approximately half of the enzyme active site. To model an extended β-1,4-1,3-cellotriose into the active site of TFsβ-glucanase-β-1,4-1,3-cellotriose complex, a cellobiose numbered $+1$ to $+2$ was added and connected (linked) to β-1,4-1,3-cellotriose [16]. All model constructions and analyses were performed using TURBO-FRODO [20].

Modeling CLHA1 into the active site of barley β-glucanase

Molecular coordinates, minus water molecules, from the crystal structure of barley β-glucanase, PDB code 1AQ0 [15], were used for this study. Firstly, residues Glu56 and Glu60 of TFsβ-glucanase-β-1,4-1,3-cellotriose complex structure (PDB 1ZM1) [16] were superimposed on the active site of the relative position of catalytic residues Glu232 and Glu93 of barley β-glucanase, respectively. A β-1,4-1,3-cellotriose (subunit -3 to -1) molecule was then built and modeled into the active site of barley β-glucanase. Secondly an extended β-1,4-1,3-cellotriose numbering $+1$ to $+3$ was constructed and modeled into the active site of barley β-glucanase to generate the CLHA1 structure. All superimpositions were performed with the Swiss-Pdb viewer (http://www.expasy.org/spdbv/).

Modeling CLHA2 into the active site of banana endo-β-1,3-glucanase

The TFsβ-glucanase-β-1,4-1,3-cellotriose complex with residues Glu56/Glu60 was firstly superimposed on the relative position of the catalytic residues Glu236/Glu94 of banana β-1,3-glucanase (PDB 2CYG) [19]. A cellobiose subunit -2 to -1 with a β-1,3-glycosidic linkage from β-1,4-1,3-cellotriose was then used as a starting template to model CLHA2 of banana endo-β-1,3-glucanase. Next, glucose rings 4 and 5 of the β-1,3-heptaose from the carbohydrate-binding module (CBM) complex (PDB 1QUI) [21] were superimposed on the previously built cellobiose (-2 to -1) to generate subunit -3 of CLHA2. Glucose rings 2 and 3 of β-1,3-heptaose were then superimposed on -3 and -2 of CLHA2 to build subunit $+1$ of CLHA2. Finally, subunits $+2$ and $+3$ of CLHA2 were constructed one by one in the same manner as subunit $+1$.

Molecular minimization, docking and dynamic equilibration

Molecular minimizations were carried out on all the above modeled carbohydrates with β-glucanases and banana β-1,3-glucanase complexes using the CNS [22] model-minimize program with conjugate gradient minimization with no experimental energy term. All molecular minimization

runs for the above three complexes were set up using the same protocol with 100 steps and a non-bonded cutoff of 13 Å. Molecular dynamic calculations were performed with the Accelrys Discovery Studio (DS 1.6, http://www.accelrys.com) and the CHARMm forcefield. Before molecular dynamic calculations, the constructed CLPA, CLHA1, and CLHA1 were analyzed by a docking process to find the best substrate binding sites in the individual enzymes, and then water molecules were added to the complexes. In an explicit solvation of 20 Å radius under periodic boundary conditions in a truncated octahedral water box, 5,840, 6,589, and 4,961 water molecules were added to TFsβ-glucanase-CLPA, barley β-glucanase-CLHA1, and banana endo-β-1,3-glucanase-CLHA2, respectively. These models were further analyzed using an Accelrys DS standard dynamic cascade protocol including the following steps: minimization, heating, equilibration, and production. Two 500-step minimizations were performed, one using the robust steepest-descent algorithm to resolve any bad contacts, and another using the adopted basis Newton–Raphson (ABNR) method to ensure that a low energy staring point was supplied to subsequent dynamic stages. In addition, the system was slowly heated from 50 to 310 K over a period of 10 ps. The system was then equilibrated at the target temperature for 10 ps before the production run was started. The product was collected at a final step of 100 ps. Finally, the system without solvent was subjected to 1,000-step minimization using the ABNR method. A dihedral restraint for glucose ring and distance restraint for the C1 atom of the −1 subunit substrate and the oxygen atom of the proposed catalytic residues were applied through the dynamic calculations.

Results and discussion

TFsβ-glucanase-CLPA complex structure

The overall structure of the TFsβ-glucanase-β-1,4-1,3-cellotriose structure with a cellobiose (TFsβ-glucanase-CLPA complex) is shown in Figs. 1a and 2a. CLPA with five glucose residues, numbered −3 to +2, contained continuous β-1,4, β-1,3, β-1,4, and β-1,4 glycosidic bonds. The glycosidic bonds between glucose residues −3 and −2, −1 and +1, +1 and +2 were β-1,4 linkages, whereas the bonds between glucose residues −2 and −1 were β-1,3 linkages. The bonds between glucose residues +1 and +2 could adopt either β-1,4 linkages or β-1,3 linkages (data not shown). The conformation of CLPA can be described by the torsion angles ϕ and ψ across the glycosidic bond: the ϕ and ψ dihedral angles at β-1,3 linkages were defined by O5–C1–O–C3 and C1–O–C3–C2, while ϕ and ψ at β-1,4 linkages were defined by O5–C1–O–C4 and C1–O–C4–C3, respectively. CLPA conformation of dihedral angles ϕ and ψ is summarized in Table 1a.

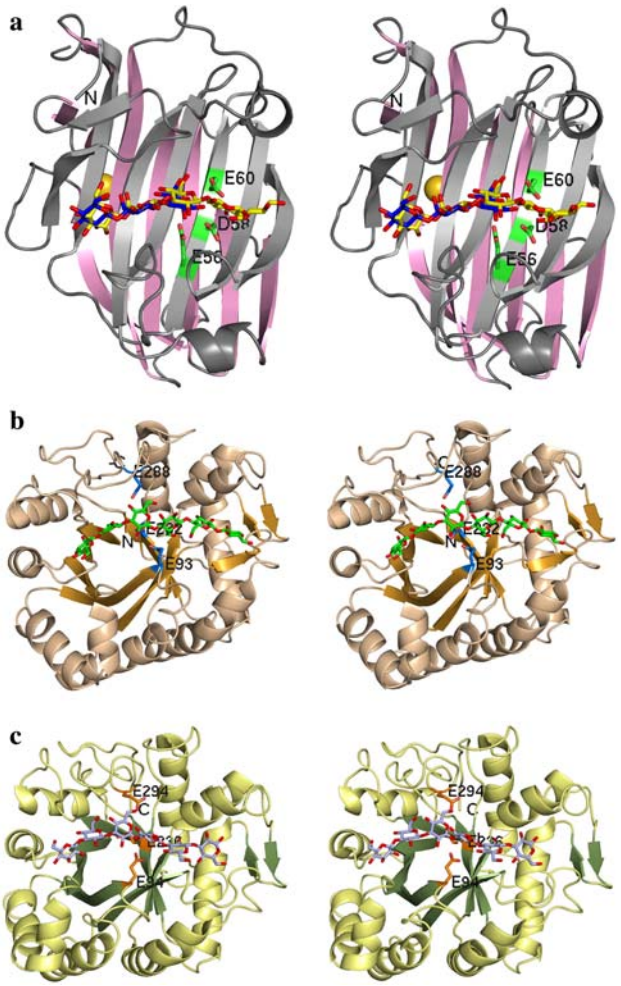

Fig. 1 Ribbon drawing of three complexes: All color figures presented in this paper were drawn with PyMol (http://www.pymol.org). (**a**) The complex crystal structure of TFsβ-glucanase-β-1,4-1,3-cellotriose with an extended cellobiose. Ribbon drawing of the overall TFsβ-glucanase-CLPA complex with glucose residues −3 to +2 (from left to right) shown as a yellow and red ball-and-stick model. β-1,4-1,3-Cellotriose is also shown as a blue and red ball-and-stick model for comparison. The complex structure is orientated so that the reducing end of CLPA is on the top right of the protein molecule with two eight β-stranded antiparallel β-sheets, one in front (grey) and another behind (pink). The key catalytic residues Glu56, Asp 58, and Glu60 are shown in green. The calcium ion is shown as a gold ball on the convex site of the protein molecule. (**b**) The overall barley β-glucanase-CLHA1 complex with glucose residues −3 to +3 (from left to right) shown as a green and red ball-and-stick model. The complex structure with β-strands (orange) and α-helix (light-brown) is shown. The key catalytic residues Glu93, Asp 232, and Glu288 are shown as a blue and red ball-and-stick model. (**c**) The overall banana β-1,3-glucanase-CLHA2 complex with glucose residues −3 to +3 (from left to right) shown as a light-blue and red ball-and-stick model. The complex protein molecule with β-strands (green) and α-helix (lemon) is shown. The key catalytic residues Glu94, Glu236, and Glu294 are shown as an orange ball-and-stick model

The structural differences before and after computational molecular dynamics are small with an average

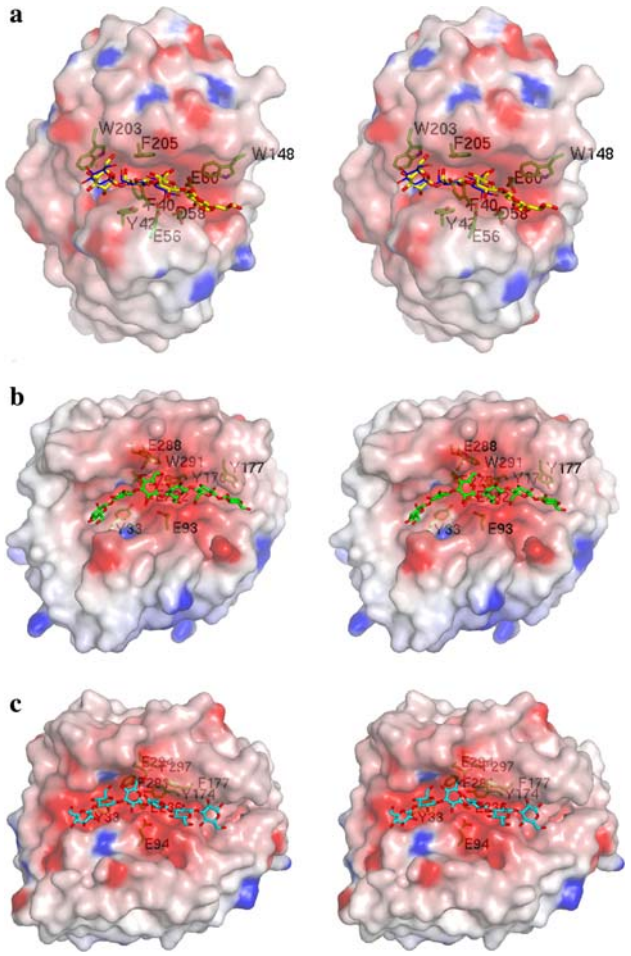

Fig. 2 (**a**) The molecular surface of TFsβ-glucanase with CLPA and β-1,4-1,3-cellotriose. The key catalytic residues Glu56, Asp 58, and Glu60 as well as aromatic residues Tyr42, Phe205, Trp141, Trp148 and Trp203 are shown. CLPA exhibits a concave-shaped conformation in the structural model. The picture is color-coded to indicate electrostatic potential, i.e., blue and red correspond to positively and negatively charged areas, respectively, and white indicates areas of neutral charge. Glucose residues −2 to +1 of substrate are buried deeply in the enzyme cleft and glucose residues +2 and +3 of the substrate are bound at a shallower position in the active cleft. (**b**) The molecular surface of barley β-glucanase with CLHA1 model**.** The key catalytic residues Glu93, Asp 232, and Glu288 as well as aromatic residues Tyr33, Tyr170, Tyr177, Phe275, and Trp291 are shown. (**c**) The molecular surface of banana β-1,3-glucanase and CLHA2 model. The key residues Glu94, Asp 236, and Glu294 as well as aromatic residues Tyr33, Tyr174, Phe177, Phe281, and Trp297 are shown

r.m.s.d. of 0.4 Å for all 233 corresponding Cα atoms. There were 23 hydrogen bonds (<3.5 Å) found in the TFsβ-glucanase-CLPA complex between CLPA and 13 residues, and five van der Waals stacking interactions with residues Phe40, Tyr42, Trp148, Phe250, and Trp203. The overall hydrogen bonding and van der Waals stacking interactions between the amino acid residues and CLPA are shown in Fig. 3a. The glucose residue −3 formed three hydrogen bonds with residues Asn44 and Thr204, and one van der Waals stacking interaction with Trp203. Glucose residue −2 made two hydrogen bonds with residue Glu11. In addition, glucose residue −2 was sandwiched between two aromatic residues, Tyr42 and Phe205. There were seven hydrogen bonds identified between glucose residue −1 and residues Ser38, Glu56, Glu60, Asn139 and Trp141, and one van der Waals stacking interaction with Phe40. The glucose residue +1 made eight hydrogen bonds with four amino acids Asp58, Glu60, Gln70, and Asn72, and one van der Waals stacking interaction with Trp148. There were also three hydrogen bonds between glucose residue +2 and amino acids Gln81 and Glu85.

Barley β-glucanase-CLHA1 complex structure

Barley β-glucanase folded into a $(\beta/\alpha)_8$ barrel, forming an open pocket active site at the end of eight parallel β-strands, as shown in Figs. 1b and 2b with the modeled CLHA1 bound to the active pocket of β-glucanase. The order of glycosidic bonds of CLHA1, numbered −3 to +3, was the same as that in CLPA, with β-1,3 linkages between glucose residues −2 and −1 and residues +2 and +3, and β-1,4 linkages between glucose residues −3 and −2, −1 and +1, +1 and +2 . CLHA1 dihedral angles ϕ and ψ are summarized in Table 1a.

The structural differences before and after molecular dynamic calculation of all the 305 corresponding Cα atoms and carbohydrate CLHA1, with an average r.m.s.d. of 1.37 Å, are shown in Fig. 3b. On the basis of this barley β-glucanase-CLHA1 model, we found 26 hydrogen bonds (<3.5 Å) between CLHA1 and barley β-glucanase active site 16 residues and two van der Waals stacking interactions with residues Tyr33 and Tyr177 (Fig. 3b). The glucose residue −3 formed five hydrogen bonds with residues Tyr5, Tyr33, and Ala34. There were five hydrogen bonds between glucose residue −2 and residues Ser8, Tyr33, Glu280, and Lys283, and one van der Waals stacking interaction with Tyr33. Seven hydrogen bonds were present between glucose residue −1 and residues Asn92, Glu93, Tyr170, Lys283 and Glu288. The glucose residue +1 made five hydrogen bonds with amino acids Glu93, Ser128, Gln129 and Asn168. Two hydrogen bonds were found between glucose residue +2 and Ser128 and Gln129, while glucose +3 had two hydrogen bonds with Leu132 and Tyr177, and one van der Waals stacking interaction with Tyr177.

Banana β-1,3-glucanase-CLHA2 complex structure

The modeled complex of CLHA2 bound to the active pocket of banana β-1,3-glucanase, based on Glu94 and Glu236 being the catalytic residues, is shown in Figs. 1c and 2c. CLHA2 dihedral angles ϕ and ψ are summarized in

Table 1 Carbohydrate conformation of ϕ, ψ dihedral angles in β-1,3 or β-1,4 oligosaccharides. Carbohydrate conformation of dihedral angles ϕ, ψ in (a) β-1,3-1,4 mixed structures and (b) β-1,3 or β-1,4 complex structures

Protein (GHF)	(ϕ, ψ)				
	β-1,4 $-3 \rightarrow -2$	β-1,3 $-2 \rightarrow -1$	β-1,4 $-1 \rightarrow +1$	β-1,4 $+1 \rightarrow +2$	β-1,3 $+1 \rightarrow +2$
(a) β-1,3-1,4 mixed structures					
TFsβ-glucanase-β-1,4-1,3-cellotriose (pdb:1ZM1)	(−77, 111)	(−78, −126)			
	(−80, 117)	(−71, −125)			
TFsβ-glucanase-CLPA	(−68, 128)	(−72, −122)	(−163, 117)	(−66, 110)	
Barley-CLHA1	(−85, 60)	(−50, −94)	(−30, 99)	(−82, 153)	(−132, −122)
	β-1,3	β-1,3	β-1,3	β-1,3	β-1,3
Banana-CLHA2	(−121, −123)	(−52, −130)	(17, −166)	(−55, −133)	(−37, −127)

1ECE[a] β-1,4	4TF4[b] β-1,4	1JS4[b] β-1,4	1IA7[c] β-1,4	1U0A[d]		4ENG[e] β-1,4	1GU3[f] β-1,4	1GUI[f] β-1,3
				β-1,3	β-1,4			
(b) β-1,3 or β-1,4 complex structures								
−100, 96	−76, 119	−76, 112	−76, 113	−74, −127	−57, 116	−81, 109	−45, 134	−82, −61
					−34, 116			
−25, 107	−75, 107	−72, 89		−79, −125	−88, 137	−68, 133	−58, 107	−94, −135
					−33, 109			
−87,126	−74, 111			−74, −130	−52, 122	−69, 115	−87, 88	−120, −118
					−28, 109			
	−71, 117			−77, −124	−55, 121	−93, 102	−81, 112	−63, −120
					−43, 114			
								−115, −134
GHF5	GHF9	GHF9	GHF9	GHF16		GHF45	CBM4	CBM4

Key to references: [a] [31]; [b] [32]; [c] [33]; [d] [17]; [e] [34]; [f] [21]

Table 1a. The structural differences before and after computational molecular dynamic calculation of all the 312 corresponding Cα atoms and carbohydrate CLHA2, with an average r.m.s.d. of 1.21 Å, are shown in Fig. 3c. There were 16 hydrogen bonds (<3.5 Å) between CLHA2 and 11 residues in the active site of banana β-1,3-glucanase, and two van der Waals stacking interactions with Tyr33 and Phe177 (Fig. 3c). The glucose residues −3 formed two hydrogen bonds with residue Ser57. The glucose residue −2 had one hydrogen bond with residue Lys289 and one van der Waals stacking interaction with Tyr33. There were two hydrogen bonds between glucose residue −1 and residues Asn93 and Glu94. Glucose +1 had three hydrogen bonds with residues Glu94, Asn172, and Glu294, which also showed one van der Waals stacking interaction with Phe177. Glucose residue +2 had one hydrogen bond with residue Thr133, and glucose residue +3 made six hydrogen bonds with residues Thr133, Gly134, Ser139, Phe177, and Asn182. A similar observation of glucose residue subunits −2 to +1 in a banana β-1,3-glucanase structure with a modeled cellotriose was also reported recently by Receveur-Brechot and co-workers [19]. The residues Asn93, Glu294, and Tyr174 were putatively involved in substrate binding and the aromatic residues Tyr33, Phe177, Phe281, and Phe297 stacked onto the sugar rings of the substrate.

Comparison of active sites of TFsβ-glucanase and barley β-glucanase

Although the amino acid sequences and overall fold of TFsβ-glucanase and barley β-glucanase are completely different, the two β-glucanases share some common features in binding and cleavage of lichenan and β-D-glucan. The active site of TFsβ-glucanase is approximately 24 Å × 7 Å × 9.5 Å, and composed of 20 amino acids (Fig. 3a) (<4.0 Å), whereas barley β-glucanase's active site is approximately 30 Å × 10 Å × 12 Å, and is composed of 19 amino acids (<4.0 Å) (Fig. 3b). The surface area buried at the interface of CLPA and TFsβ-glucanase was 1,174 Å^2, and 1,429 Å^2 for CLHA1 and barley β-glucanase. The glucose rings −3 to +1 in TFsβ-glucanase-CLPA had van der Waals contacts with the aromatic residues Trp203, Tyr42, Phe205, Phe40, and Trp148 (Fig. 1c),

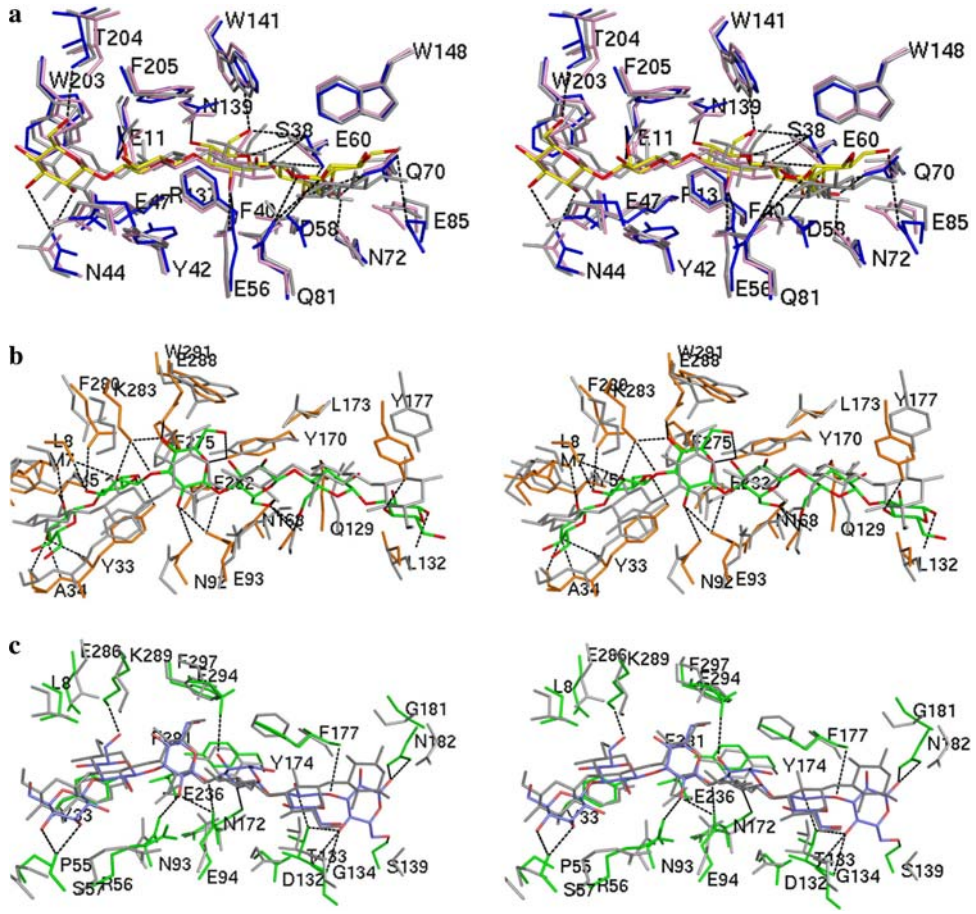

Fig. 3 Stereo view of the active sites. (**a**) The superimposed active site of crystal structure TFsβ-glucanase-β-1,4-1,3-cellotriose complex (pink), before (grey) and after (blue) molecular dynamic calculation of TFs β-glucanase-CLPA complex. The 23 hydrogen bond (<3.5 Å) network between CLPA and residues Glu11, Ser38, Asn44, Glu56, Asp58, Glu60, Gln70, Asn72, Gln81, Glu85, Asn139, Trp141, and Thr204, and five van der Waals stacking interactions with residues Phe40, Tyr42, Trp148, Phe250, and Trp203 are shown. (**b**) The superimposed active site of barley β-glucanase-CLHA1 complex before (dark grey) and after (orange) molecular dynamic calculation. The 26 hydrogen bond (<3.5 Å) network between CLHA1 and residues Tyr5, Ser8, Tyr33, Ala34, Asn92, Glu93, Ser128, Gln129, Leu132, Asn168, Leu173, Glu232, Glu280, and Glu288 of barley β-glucanase, is shown. The glucose rings −2 and +3 made two van der Waals stacking interactions with residues Tyr33 and Tyr177, respectively. (**c**) The superimposed active site of banana β-glucanase-CLHA2 complex before (grey) and after (green) molecular dynamic calculation. The 16 hydrogen bond (<3.5 Å) network between CLHA2 and residues Ser57, Asn93, Dlu94, Thr133, Gly134, Ser139, Asn172, Phe177, Asn182, Lys289, and Glu294 of banana β-1,3-glucanase, is shown in the active site. The glucose rings −2 and +1 made two van der Waals stacking interactions with residues Tyr33 and Phe177, respectively. The color of CLPA, CLHA1, and CLHA2 is like shown in Fig. 1

whilst the glucose rings −2 and +3 made van der Waals contacts with the aromatic residues Tyr33 and Tyr177, respectively, in barley β-glucanase-CLHA1 (Fig. 2c). These aromatic residues in both enzymes may play an important structural role in stabilizing glucose rings. Those mutants with replacement of aromatic residues Trp141, Trp148, and Trp203 [23], or of Phe40, Tyr42, and Phe205 (data not published) in TFsβ-glucanase exhibited low substrate binding activity and decreased stabilization of active site residues compared to the wild type. The glucose rings −3 to +1 in TFsβ-glucanase-CLPA were buried deeper in the active cleft (Fig. 1b) than those in the active site pocket of barley β-glucanase-CLHA1 (Fig. 2b).

Comparison of active sites of barley β-glucanase and banana β-1,3-glucanase

The surface area buried at the interface of banana β-1,3-glucanase and CLHA2 was 1,381 Å^2. The active site of β-1,3-glucanase was approximately 30 Å × 10 Å × 12 Å, comprising 18 amino acids (Fig. 3c) (<4.0 Å). There were seven conserved residues found in both enzymes' active sites, Tyr33/Tyr33, Asn92/Asn93, Glu93/Glu94, Tyr170/Tyr174, Glu232/Glu236, Phe275/Phe281, and Glu288/Glu294, which were involved with substrate binding (Fig. 3b and c). The above-mentioned region of 7 conserved residues displayed similar topographies in both

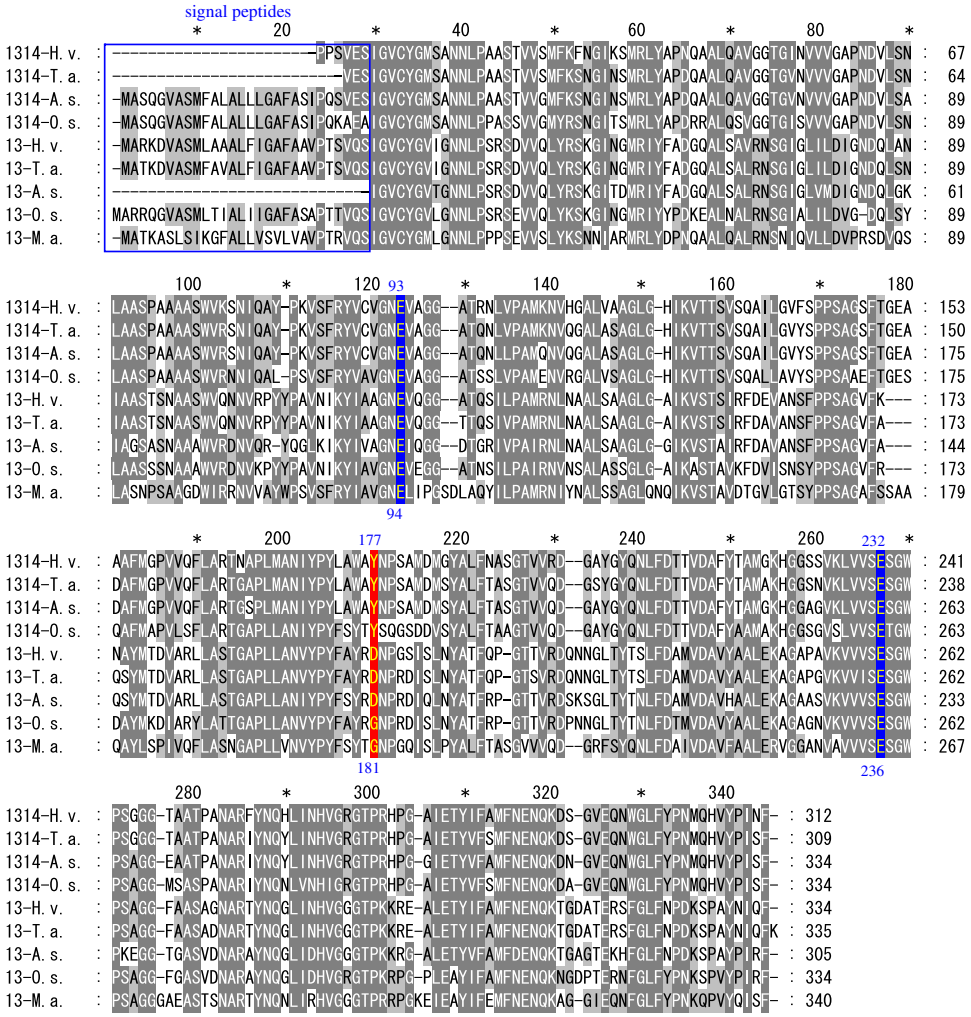

Fig. 4 Amino acid sequence alignment of plant β-1,3-glucanases and β-1,3-1,4-glucanases. The primary sequence of barley *Hordeum vulgare* β-1,3-1,4-glucanase (1314-H.v., UniProt:P12257) [14] is compared with those of wheat *Triticum aestivum* β-1,3-1,4-glucanase (1314-T.a., UniProt: Q07556) [25], oat *Avena sativa* β-1,3-1,4-glucanase (1314-A.s., UniProt:Q42518) [26], and rice *Oryza sativa* β-1,3-1,4-glucanase (1314-O.s., UniProt:Q40686) [27], as well as barley *Hordeum vulgare* β-1,3-glucanase (13-H.v., UniProt:Q64938) [14], wheat *Triticum aestivum* β-1,3-glucanase (13-T.a., UniProt:O82716) [28], oat *Avena sativa* β-1,3-glucanase (13-A.s., UniProt:Q9LLS8) [29], rice *Oryza sativa* β-1,3-glucanase (13-O.s., UniProt:Q8W4V0) [30], and banana *Musa acuminata* β-1,3-glucanase (13-M.a., UniProt:O22317) [19]. The alignment was optimized by introducing gaps, denoted by dashes. The N-terminal signal peptide from residues 1 to 30 are surrounded by a blue box. The conserved catalytic residues of Glu232/Glu93 in barley and other β-1,3-1,4-glucanases and Glu236/Glu94 in banana and other β-1,3-glucanases are highlighted in a pair of blue boxes with yellow text. The residue Tyr177 in barley β-1,3-1,4-glucanase, the equivalent tyrosines in other β-1,3-1,4-glucanases, as well as the glycine or aspartate residue in other β-1,3-glucanases are highlighted in a red box with yellow text

enzymes when accommodating glucose rings -2 and -1, containing the same β-1,3 glycosidic linkage, of CLHA1 and CLHA2. The two conserved Tyr33 residues in both enzymes exhibited van der Waals stacking interactions with glucose ring -2 of both CLHA1 and CLHA2. The four residues Asn92/Asn93, Glu93/Glu94, Glu232/Glu236, and Glu288/Glu294 also made hydrogen bonds with their respective substrate glucose rings at position -1, with the aromatic residues Tyr170/Tyr174, Phe275/Phe281, and Trp291/Phe297 structurally supporting the -1 glucose rings in barley β-glucanase and banana β-1,3-glucanase. However, the residues around glucose rings $+1$ to $+3$ exhibited low homology, with the residues Leu173 and Tyr177 in barley β-glucanase and Phe177 and Gly181 in banana β-1,3-glucanase above glucose rings $+1$ to $+3$. These differences may result in a wider space for glucose rings $+1$ to $+3$ in the binding site of banana β-1,3-glucanase (Fig. 3b and c).

Our CLHA1 and CLHA2 models offer a possible explanation for why banana β-1,3-glucanase but not barley β-glucanase is able to cleave β-1,3-glucan, although both enzymes share high homology regarding amino acid sequence and active site folds. In barley β-glucanase, the glucose ring $+3$ of CLHA1 was found to make a van der

Waals stacking interaction with Tyr177. In banana β-1,3-glucanase, the glucose ring +3 of CLHA2 formed six hydrogen bond interactions with Thr133, Gly134, Ser139, Phe177, and Asn182 (Fig. 3c), but had no van der Waals stacking interaction with aromatic residues. Instead, Gly181 is in an equivalent structural position to residue Tyr177 of barley β-glucanase (Fig. 3c). Therefore the location of the bulky Tyr177 in barley β-glucanase may restrain the orientation of the glucose ring +3 and also limit the carbohydrate conformation upon substrate binding in the active site of barley β-glucanase. This means that Tyr177 may be involved in determining the specificity of barley β-glucanase for a β-1,3 linkage between glucose rings +2 and +3 after the β-1,4 linkage between glucose rings +1 and +2. Moreover, from a structural point of view, when we tried to model CLHA2 into the active site of barley β-glucanase to analyse the role of residue Tyr177, such attempts failed because the glucose rings +2 and +3 of CLHA2 were found to collide with Tyr177, further confirming the steric hindrance role Tyr177 may play in defining substrate specificity in barley β-glucanase. An alignment analysis of the primary sequence of barley β-glucanase with other plant β-1,3-glucanases and β-1,3-1,4-glucanases revealed that the tyrosine is an important conserved residue in all β-1,3-1,4-glucanases (Fig. 4). In contrast, in the various known β-1,3-glucanases, the equivalent structural position to the tyrosine residue is occupied either by glycine or aspartate (Fig. 4).

Structures of CLPA, CLHA1 and CLHA2

Differences in the fold shape and residues of active sites in TFsβ-glucanase, barley β-glucanase and banana β-1,3-glucanase created particular substrate binding topographies for CLPA, CLHA1 and CLHA2. The CLPA in TFsβ-glucanase-CLPA complex was deformed from its original linear shape, and needed to be bent $\sim 30°$ at the cleavage site (Fig. 2a) into a V-shape, in order to bind to the active site of TFsβ-glucanase, whilst barley β-glucanase presented a shallow groove (Fig. 2b) that did not require CLHA1 to undergo much deformation upon binding. CLHA2 maintained a U-shape upon binding to the active site of banana β-1,3-glucanase, similar to that found in the carbohydrate-binding module 4 (CBM4) complex (PDB 1QUI) [21]. The conformations of CLPA, CLHA1, and CLHA2 bound to their respective enzymes in this study are summarized in Table 1a. The torsion angles ϕ and ψ of CLPA, CLHA1, and CLHA2 are similar to those of other β-1,3 and β-1,4 oligosaccharide glycosidic linkages (Table 1b) found in GHFs 5, 9, 16, and 45 [17] and the CBM4 complex [21]. The dihedral angles ϕ/ψ at the cleavage site (β-1,4 glycosidic bond $-1 \rightarrow +1$) of CLPA in TFsβ-glucanase-CLPA complex changed from an average value of $-78/114$ [16] in a low energy region to $-163/117$ in a high energy region [24] upon CLPA binding to the active site of TFsβ-glucanase. However, the dihedral angles ϕ/ψ at the cleavage sites of CLHA1 ($-30/99$) and CLHA2 ($17/-166$) were located in low energy regions in barley β-glucanase-CLHA1 and banana β-1,3-glucanase-CLHA2 complexes. These results indicate that CLPA binds to the active site of TFsβ-glucanase through an induced-fit mechanism and thus requires more free energy to perform the reaction from a ground-state to a transition-state than for CLHA1 binding to barley β-glucanase or CLHA2 binding to banana β-1,3-glucanase.

Conclusions

Glycosyl hydrolases have unique abilities to recognize and bind their substrate carbohydrates and then cleave the specific glycosidic bond between two or more carbohydrates. The two extremely different folds adopted by GHF16 and GHF17 enzymes, β-jellyroll and $(\beta/\alpha)_8$, respectively, appear to accommodate mixed β-1,3 and β-1,4 β-D-glucans or lichenan. Comparison of the active sites of TFsβ-glucanase and barley β-glucanase in this study has revealed that TFsβ-glucanase possesses a unique and compact active site which requires induced-fit substrate binding for enzymatic cleavage.

Although the folding and active site of barley and banana enzymes are similar, they recognize and hydrolyze different glycosidic linkages of polysaccharide. Detailed structural analysis in this study of the interactions between barley β-glucanase and CLHA1 as well as banana β-1,3-glucanase and CLHA2 suggest that both enzymes may use conserved and equivalent residues, Glu232/Glu93 in barley β-glucanase and Glu236/Glu94 in banana β-1,3-glucanase, as the nucleophile/hydrogen donors (Fig. 3b and c). Our model, however, suggests that the residue Tyr177 in barley β-glucanase is also involved in recognizing and stabilizing mixed β-1,3 and β-1,4 β-D-glucans or lichenan (Fig. 2c). Taken together, our model studies shed light on how GHF16 and GHF17 β-glucanases and GHF17 banana β-1,3-glucanase individually interact with their carbohydrate substrates. What we have learnt from these enzymes in terms of enzyme active sites, polysaccharide recognition and hydrolysis may well apply to other glycosyl hydrolases which share very similar folds yet bind diverse carbohydrates, or display different folds but recognize the same glycosidic bonds.

Acknowledgements This work was supported by research grants from National Taipei University of Technology and National Science Council (NSC94-2311-B-027-001), Taipei, Taiwan, ROC.

References

1. Koshland DE (1953) Biol Rev Camb Philos Soc 28:416
2. Mayer C, Zechel DL, Reid SP, Warren RAJ, Withers SG (2000) FEBS Lett 466:40
3. Davies GJ, Ducros VMA, Varrot A, Zechel DL (2003) Biochem Soc Trans 31:523
4. Davies GJ, Gloster TM, Henrissat B (2005) Curr Opin Struc Biol 15:637
5. Shaikh FA, Withers SG (2008) Biochem Cell Biol 86:169
6. Anderson MA, Stone BA (1975) FEBS Lett 52:202
7. Keitel T, Simon O, Borriss R, Heinemann U (1993) Proc Natl Acad Sci USA 90:5287
8. Juncosa M, Pons JDT, Querol E, Planas A (1994) J Biol Chem 269:14530
9. Hahn M, Keitel T, Heinemann U (1995) Eur J Biochem 232:849
10. Viladot J-L, de Ramon E, Durany O, Planas A (1998) Biochemistry 37:11332
11. Chen J-L, Tsai L-C, Wen T-N, Tang J-B, Yuan HS, Shyur L-F (2001) J Biol Chem 276:1789
12. Tsai L-C, Shyur L-F, Lee S-H, Lin S-S, Yuan HS (2003) J Mol Biol 330:607
13. Chen L, Fincher GF, Hoj PB (1993) J Biol Chem 268:13318
14. Varghese JN, Garrett TPJ, Colman PM, Chen L, Hoj PB, Fincher GB (1994) Proc Natl Acad Sci USA 91:2785
15. Müller JJ, Thomsen KK, Heinemann U (1998) J Biol Chem 273:3438
16. Tsai L-C, Shyur L-F, Cheng Y-S, Lee S-H (2005) J Mol Biol 354:642
17. Gaiser OJ, Piotukh K, Ponnuswamy MN, Planas A, Borriss R, Heinemann U (2006) J Mol Biol 357:1211
18. Jenkins J, Lo Leggio L, Harris G, Pickersgill R (1995) FEBS Lett 362:281
19. Receveur-Brechot V, Czjzek M, Barre A, Roussel A, Peumans WJ, Van Damme EJM, Rouge P (2006) Proteins 63:235
20. Roussel A, Cambillau C (1992) The TURBO-FRODO graphics package graphics geometry partners directory, vol 81. Silicon Graphics, Mountain View, CA
21. Boraston AB, Nurizzo D, Notenboom V, Ducros V, Rose DR, Kilburn DG, Davies GJ (2002) J Mol Biol 319:1143
22. Brunger AT, Adams PD, Clore GM, Delano WL, Gros P, Grosse-Kunstleve RW, Jiang J-S, Kuszewski J, Nilges N, Pannu NS, Read RJ, Rice LM, Simonson T, Warren GL (1998) Acta Cryst D 54:905
23. Cheng H-L, Tsai L-C, Lin S-S, Yuan HS, Lee S-H, Shyur L-F (2002) Biochemistry 41:8759
24. Nelson D, Cox M. Lehninger's principles of biochemistry: Freeman; chapter 7 carbohydrates and glycobiology, Fig 7–20
25. Lai D, Høj P, Fincher G (1993) Plant Mol Biol 22:847
26. Yun S, Martin D, Gengenbach B, Rines H, Somers D (1993) Plant Physiol 103:295
27. Simmons CR, Litts JC, Huang N, Rodriguez RL (1992) Plant Mol Biol 18:33
28. Dudler R (1998) EMBL/GenBank/DDBJ databases
29. Martin DJ, Somers DA (2004) J Cereal Sci 39:265
30. Akiyama T (2001) EMBL/GenBank/DDBJ databases
31. Sakon J, Adney W, Himmel M, Thomas S, Karplus P (1996) Biochemistry 35:10648
32. Sakon J, Irwin D, Wilson DB, Karplus PA (1997) Nat Struct Biol 4:810
33. Parsiegla G, Belaich A, Belaich J-P, Haser R (2002) Biochemistry 41:11134
34. Davies GJ, Tolley SP, Henrissat B, Hjort C, Schulein M (1995) Biochemistry 34:16210